Serrano Aroca, A.; Monleón Pradas, M.; Gómez Ribelles, JL.; Rault, J. (2015). Thermal analysis of water in reinforced plasma-polymerised poly(2-hydroxyethyl acrylate) hydrogels. European Polymer Journal. 72:523-534.

Thermal analysis of water in reinforced plasma-polymerised poly(2-hydroxyethyl acrylate) hydrogels

A. Serrano Aroca[1,*], M. Monleón Pradas[2], J.L. Gómez Ribelles[2] , J. Rault[3]

[1] *Departamento de Ciencias Aplicadas y Tecnológicas. Facultad de Veterinaria y Ciencias Experimentales. Universidad Católica de Valencia San Vicente Mártir. C/ Guillem de Castro 94, 46001-Valencia, Spain*

[2]*Center for Biomaterials and Tissue ·Engineering, Universitat Politècnica de València. Camí de Vera s/n E- 46071 València, Spain.*

[3]*Laboratoire de Physique des Solides, Université Paris-Sud XI, Bât.510, C.N.R.S., 91405 Orsay cedex, France.*

[*] *To whom correspondence should be addressed* angel.serrano@ucv.es

Thermal analysis of water in reinforced plasma-polymerised poly(2-hydroxyethyl acrylate) hydrogels

A. Serrano Aroca[1,*], M. Monleón Pradas[2], J.L. Gómez Ribelles[2] , J. Rault[3]

[1] *Departamento de Ciencias Aplicadas y Tecnológicas. Facultad de Veterinaria y Ciencias Experimentales. Universidad Católica de Valencia San Vicente Mártir. C/ Guillem de Castro 94, 46001-Valencia, Spain*

[2]*Center for Biomaterials and Tissue ·Engineering, Universitat Politècnica de València. Camí de Vera s/n E- 46071 València, Spain.*

[3]*Laboratoire de Physique des Solides, Université Paris-Sud XI, Bât.510, C.N.R.S., 91405 Orsay cedex, France.*

Abstract

Thermal analysis of water in reinforce hydrogels of plasma-polymerised poly(2-hydroxyethyl acrylate) (*pl*PHEA) grafted onto macroporous poly(methyl methacrylate) (PMMA) are explained in a simple thermodynamic framework based on the transition diagram. Water in bulk PHEA was also analysed for comparison with *pl*PHEA. These two hydrophilic polymers were prepared with a broad range of water mass fractions from 0.05 to 0.72. Thermal transition diagrams of water/PHEA and water/*pl*PHEA were determined showing less undercooling of water crystallisation in *pl*PHEA than in PHEA. Kinetics of water crystallisation for high and low water contents were studied in both hydrophilic systems following several thermal treatments. Water crystallises much faster in *pl*PHEA than in PHEA for high water contents. For low water contents, crystallisation becomes possible holding at –30ºC for some time due to water segregation in both PHEA systems. However, much less water is segregated from the water/*pl*PHEA mixture due to the influence of the hydrophobic component.

Keywords: hydrogels, *pl*PHEA, poly(methyl methacrylate), thermal analysis, kinetics of crystallisation.

1. Introduction

Reinforce hydrogels of plasma-polymerised poly(2-hydroxyethyl acrylate) (*pl*PHEA) grafted onto macroporous poly(methyl methacrylate) (PMMA) can form a resistant polymer hydrogel when water is absorbed. The 'state' of water and its influence on the hydrogel's properties thus become of primary importance.

The 'state' of water in a swollen hydrogel has been frequently classified into *free*, *freezable bound* and *non-freezing water*. *Free water* and *non-freezing water* are the two extremes of the continuum water 'states' in a hydrogel [1]. *Free or freezing water* is defined as the water which has the same phase transition temperature as bulk water [2]. *Freezable bound water* is the water having a phase transition temperature lower than 273 K. This depression is usually ascribed to the weak interaction of the water with the polymer chains and/or the capillary condensation in the hydrogel [3,4]. *Bound or non-freezing water* is defined as the water, which has no detectable phase transition from 273 to 200K [5]. These water molecules would be strongly associated with the polymer network through hydrogen bonding. Specific strong interactions do not allow the migration of water molecules to the growing crystal phase. Thus, a certain amount of water remains homogeneously mixed with the polymer chains.

Thermal transitions in the polymer hydrogels studied in this paper are explained in a simple thermodynamic framework based on a temperature-composition diagram where the temperature of the transitions is plotted versus water content. Thermal analysis of water in hydrophilic polymer networks [6-8] and hydrophilic/hydrophobic interpenetrated polymer networks (IPNs) [9,10] have been

done in the past. However, no studies can be found in the literature about thermal analysis of water in hydrophilic/hydrophobic systems of plasma-polymerised coatings grafted onto macroporous substrates.

If the amount of solvent does not exceed a certain limit, a polymer hydrogel can be considered as a homogeneous mixture of two molecular species at room temperature: the dry polymer and the solvent. The temperature-composition diagram of this mixture is composed of three curves: T_m, T_c and T_g. The first two curves T_m and T_c define the melting and crystallisation processes of the solvent in the mixture respectively. The curve T_g indicates the composition dependence of the glass transition of the swollen polymer hydrogel. Much effort has been made to understand the composition dependence of the glass transition temperature of a binary glass-forming system [11-13]. These ideas can be applied to the polymer-water mixture in a PHEA hydrogel. The glass transition temperature curve of a hydrogel (T_{gh}) can be described by Fox's[11] and Couchman-Karasz's [12] equations. The Thermodynamics of binary systems predicts that the melting temperature of the solvent will experience a decrease, the so-called cryoscopic depression, with respect to the melting temperature of the pure component. Supercooling of 10-20 degrees is often observed in pure water even for cooling rates as low as 0.2 ºC/min. This happens because crystallisation needs the occurrence of two processes: the formation of crystal *nuclei* (germs) on the one hand and their growth on the other. Although a rate of cooling high enough can even prevent crystallisation and result in glassy water [14], for the experimentally common cooling rates in DSC from 1 to 20 ºC/min, a T_c = *-21ºC* is obtained [15].

The intersection of T_g with T_m and T_c defines the compositions ω'^{**} and ω'^{*} respectively. These two values divide the transition diagram in three concentration domains. (see Figure 1).

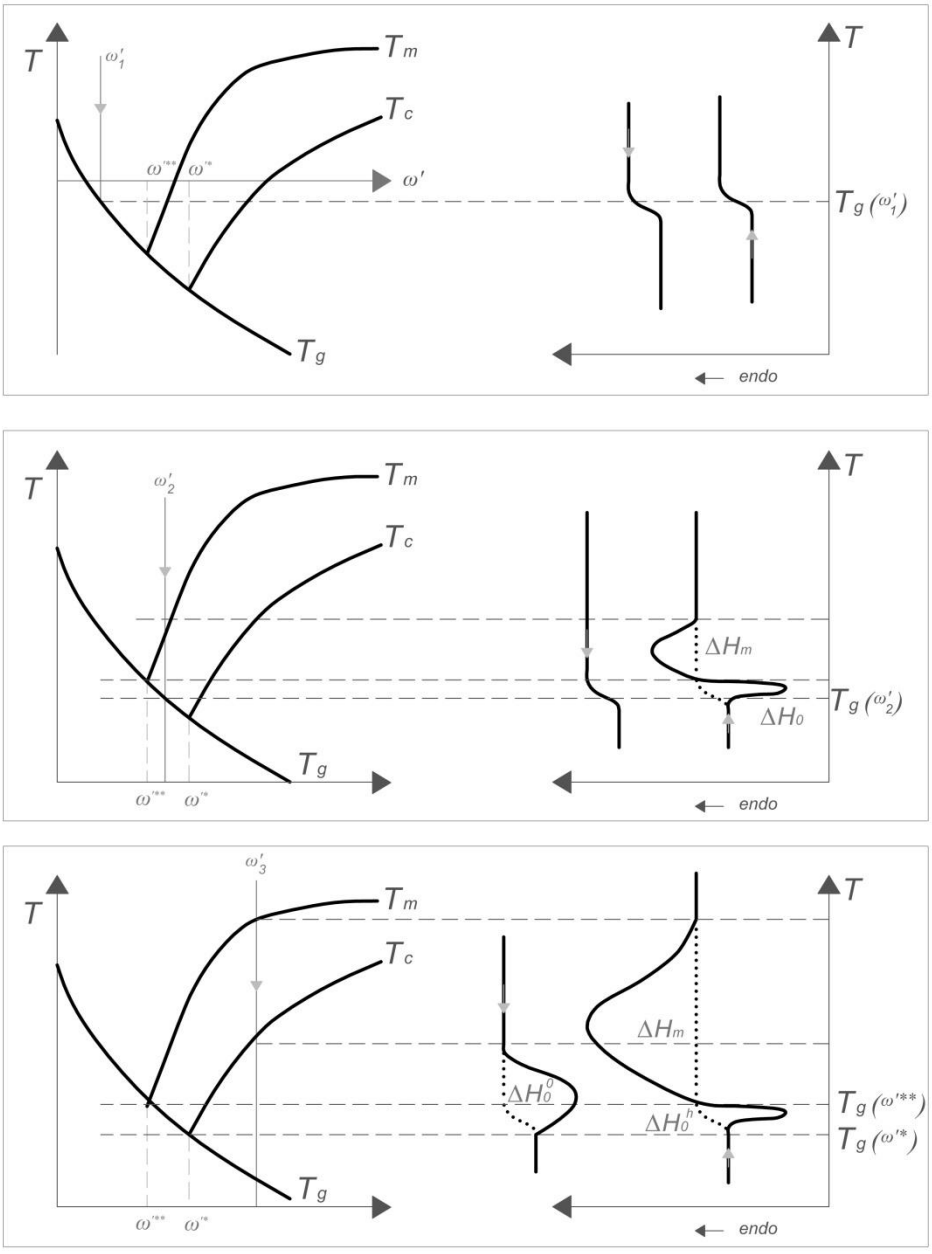

Figure 1. Expected shapes of the cooling and heating scans for polymer-water systems with compositions ω'_1, ω'_2 and ω'_3 belonging to the three different concentration domains [15].

(a) Concentration domain $\omega' < \omega'^{**}$: for a solvent concentration $\omega'_1 < \omega'^{**}$ at a temperature $T_g\ (\omega'_1)$ on cooling, the hydrogel would traverse its glass transition temperature before taking place any crystallisation. Only the glass transition of an amorphous polymer-solvent system occurs. Once the glass transition region has been reached, the mobility of the hydrogel kinetic units almost disappears and the homogeneous material remains as a glass. Physically there is no chance for solvent molecules to migrate from the vitrified polymer to form a new phase.

(b) Concentration domain $\omega'^{**} < \omega' < \omega'^{*}$: for a solvent concentration $\omega'^{**} < \omega'_2 < \omega'^{*}$, the glass transition curve is reached on cooling before crystallisation can take place and all the solvent remains *non-crystallisable* again. This can be explained by the fact that crystallisation involves the formation of a nucleus of a critical size and its subsequent growth. This second stage of growth can solely take place if the nucleus is formed. Upon cooling, nucleation of crystalline germs can occur, but growth of these germs is not possible. At $T_g(\omega'_2)$, the system is frozen as an homogeneous phase as a consequence of its glass transition, and no further thermal transitions can take place for temperatures lower than that. Then, as temperature increases, viscosity decreases and the crystal growth rate increases allowing the migration of solvent molecules from the swollen network to the embryos formed on cooling, and the solvent will crystallise on heating while still under T_m. Crystallisation causes a decrease in the solvent content present in the polymer phase. At any temperature T_t, between $T_g(\omega'_2)$ and $T_g(\omega'^{**})$, the solvent migrates from the gel to the growing crystal phase until the composition of the gel reaches a value ω'_t when crystallisation becomes impeded by the glass transition. As temperature increases, this process takes place during the heating process while $T_g(\omega'_2)$

$< T < T_g(\omega'^{**})$ and crystallisation of the solvent occurs between these two temperatures while the gel changes its composition and glass transition temperature continuously. At ω'^{**} , $T_g(\omega'^{**}) = T_m(\omega'^{**})$ and when the temperature T^{**} is passed, the phase equilibrium of solid water and the hydrogel phase of composition ω'^{**} becomes unstable with respect to an equilibrium of solid water and a hydrogel phase of composition $\omega' > \omega'^{**}$ on the T_m curve. Crystalline solvent thus begins to melt and diffuses into the hydrogel phase, increasing the latter composition until the starting ω'. Since the temperature is continuously increased, the process can be drawn following the curve T_m from $T_g(\omega'^{**})$ to $T_m(\omega'_2)$ until the starting composition ω'_2. A melting endotherm appears on the heating thermogram. Therefore, in this composition interval (ω'^{**}, ω'^{*}), no crystallisation is expected on cooling, but crystallisation and subsequent melting of water must be expected upon heating. Still, an amount of water as bound water will not crystallise $(m \cdot \omega'^{**})$. The trace of the process on the heating thermogram should thus include a first crystallisation exothermal peak followed by the melting endotherm, and the baseline jump from the beginning to the end should correspond to the heat capacity jump at the glass transition found on the cooling thermogram.

(c) Concentration domain $\omega' > \omega'^{*}$: for a solvent concentration $\omega'_3 > \omega'^{*}$, after a certain supercooling, the solvent crystallises on cooling. Crystallisation is arrested by the glass transition of the system. As the solvent segregates from the gel phase to form a crystal, the composition of the gel decreases continuously following the T_c curve until $T_g(\omega'^{*})$ is reached and a dramatic loss of mobility of the polymer chains of the gel of composition ω'^{*} takes place. The crystal phase is not able to continue growing and both

phases become frozen at lower temperatures. The amount of crystal phase will be $m\cdot(\omega'_3 - \omega'^*)$, where m is the mass of the gel of composition ω'_3. On the subsequent heating scan, the solvent will crystallise as explained before, from $T_g(\omega'^*)$ to $T_g(\omega'^{**})$ while the composition and glass transition temperature of the gel changes continuously. The amount of crystal solvent formed during heating will be $m\cdot(\omega'^* - \omega'^{**})$ independently of ω'_3. At T^{**}, the amount of ice is maximum, and the water concentration in the remaining polymer-water phase is ω'^{**}. From $T_g(\omega'^{**})$ on, the solvent will melt and diffuse following the T_m curve until the initial composition is reached.

Polymer hydrogels have many applications in biomedical engineering [16-20] due to their excellent biocompatibility and water permeation properties. However, many of their potential uses are hindered by their low mechanical strength. New families of polymers have been developed, seeking to improve the mechanical behaviour of the corresponding hydrogels. This mechanical improvement can be achieved through polymers with microphase-separated morphologies, such as block copolymers, in which hydrophobic and hydrophilic domains alternate [21] and through a binary system composed of two mixed polymers as interpenetrating polymer networks (IPNs) [22-24]. Recent studies have shown new methods to improve the mechanical properties of hydrogels increasing cross-link density by self-sorting [25] or by covalent incorporation of graphene oxide [26]. However, the mechanical properties of the hydrogel studied in this work were improved by means of a porous hydrophobic substrate where the hydrophilic component was grafted by plasma-polymerisation [27,28].

2. Experimental

2.1. Materials

Plasma-polymerised poly(2-hydroxyethyl acrylate) (*pl*PHEA) hydrophilic coatings were grafted onto macroporous poly(methyl methacrylate) (PMMA). Macroporous PMMA was allowed to adsorb 2-hydroxyethyl acrylate (HEA) monomer vapour before the plasma-polymerisation. The sample was placed inside a vacuum desiccator on a grid located on the top of a glass with liquid HEA monomer. The air was evacuated from the desiccator with the help of a vacuum pump. After that, this desiccator was placed inside an oven at 50ºC in order to accelerate the adsorption process. Once the sample had adsorbed the desired amount of monomer vapour, it was removed from the desiccator to be treated by plasma right after. The plasma treatment, performed in a Piccolo stainless steel vacuum chamber of 45 litres from Plasma-electronic GmbH (Germany), started with the evacuation of the air present inside the chamber till achieve a base pressure of 50 *Pa*. After that, 5 seconds of homogenisation and the plasma was generated by a 2.45 *GHz* generator (quartz cylinder) to produce 360 *Watts* during 110 seconds. The plasma treatment allowed the adsorbed HEA monomer to polymerise onto the macroporous PMMA sample obtaining 28.7 wt.% of *pl*PHEA. Finally, the chamber was ventilated to atmospheric pressure in 30 seconds.

The momoner HEA (from Aldrich 96% pure, stabilised with 200–600 ppm of monomethyl ether hydroquinone) was used without further purification. However, *pl*PHEA is pure because it was synthesised by plasma-polymerisation of HEA vapour.

Macroporous PMMA was synthesised by polymerisation in the presence of 70 wt.% of ethanol. The polymerisation took place under UV light with 0.2 wt.% of benzoin (from Scharlau 98% pure) as photoinitiator and 1 wt.% of ethylene glycol dimethacrylate (EGDMA, from Aldrich 98% pure) as cross-linker. The monomer (methyl methacrylate, MMA, from Aldrich 99% pure) and the cross-linking agent were purified by vacuum distillation. The polymerization took place in a mould that consisted of two glass plates with a rubber spacer that allowed the preparation of polymer sheets between 1 to 3 mm thick. The low molecular weight substances remaining in the samples after polymerization were extracted in boiling ethanol for 24 hours. Afterwards, the solvent was allowed to evaporate partially from the samples at room temperature and atmospheric pressure. This step is necessary to avoid sample cracking during the drying process. Finally, the samples were dried at 160 °C in vacuo to constant weight.

Bulk poly(2-hydroxyethyl acrylate) (PHEA) was polymerised under UV light for 24 hours with 0.2 wt.% of benzoin as photoinitiator between glass plates to form sheets approximately 1 mm thick. These samples were washed with boiling water for 24 hours and dried at 90 ºC in vacuo for three days.

2.2. Microscopy

The morphology of these composite materials was observed by Scanning Electron Microscopy (SEM). The SEM micrograph was taken in an ISIDS-130 microscope at an accelerating voltage ranging from 15 to 20 kV. The cryogenic fracture cross-section of the sample was sputtered with gold previous to observation.

2.3. Water inmersion

DSC measurements with a broad range of water mass fractions (ω'= 0.05, 0.10, 0.15, 0.20, 0.30, 0.40, 0.50 and 0.72) were performed in this work. In order to prepare each water mass fraction, the two kinds of hydrogels synthesised in this work, bulk PHEA and macroporous PMMA with 28.7 wt.% of *pl*PHEA (sample PMMA1/70E-gr-*pl*PHEA(28.7 wt.%)), were equilibrated in liquid water to constant weight for two days. After that, they were dried at room temperature the necessary time to obtain the desired water mass fraction before encapsulation.

2.4. Differential scanning calorimetry (DSC)

Differential scanning calorimetry experiments were performed in a Perkim-Elmer (Pyris 1) apparatus. The temperature of the calorimeter was calibrated with water, cyclohexane and n-octadecane. The melting heat of indium was used to calibrate the heat flow output. A cryogenic accessory with liquid nitrogen was used to cool down at low temperature.

In order to determine the transition diagram of *pl*PHEA grafted onto PMMA, the samples were subjected to a cooling scan from room temperature down to -120°C at 10°C/min, followed by a heating scan from that temperature up to 35°C at 10°C/min. The thermal transitions of water in bulk PHEA was also analysed for comparison.

Kinetics of crystallisation for high and low water contents were studied following several thermal treatments. For water mass fractions higher than ω'^{*}, water crystallises on cooling and an exothermic peak followed by an endothermic peak shows

up on heating. Bulk PHEA and PMMA1/70E-*gr-pl*PHEA(28.7 wt.%) were swollen in liquid water to obtain a water composition belonging to this domain $\omega' > \omega'^{*}$ (ω'=0.3).

In order to study the kinetics of water crystallisation for high water contents, these samples were subjected to two different thermal treatments, which will be called hereafter experiences A and B. Experience A consisted of quenching to a determined temperature T_{hold} (-10, -30, -40, -50, -65 and -70ºC) and holding at this selected T_{hold} for 15 minutes. After that, the samples were quenched to -120ºC and subsequently heated from that temperature up to 20ºC at 10 *K/min*. However, experience B consisted of quenching to -120ºC, heating from that temperature up to a determined T_{hold} (-10, -30, -40, -50, -65 and -70ºC) at 10 *K/min* and holding at this selected T_{hold} for 15 minutes. After that, the samples were quenched from T_{hold} to -120ºC. Finally, a heating scan from -120ºC up to 20ºC at 10 *K/min* was performed.

In order to study the kinetics of water crystallisation for low water contents, the samples were swollen in liquid water to obtain a water composition belonging to this domain $\omega' < \omega'^{**}$ (ω' = 0.10). The thermal treatment for this water contents consisted of subjecting the samples to a quenching from room temperature down to –30ºC and holding at that temperature during several times (1, 2, 16.7, 33.3 and 61.7 hours). After that, a quenching from –30ºC down to –50ºC followed by a first heating scan from that temperature up to 10ºC at 10 *K/min* was performed. Finally, right after this first scan, a quenching again down to –50ºC and a second heating scan from –50ºC up to 10ºC was performed at the same heating rate.

3. Results

3.1. Morphology

Figure 2 shows the interconnected structure of these composite materials by Scanning Electron Microscopy (SEM). It shows the hydrophilic coating formed onto the macroporous substrate after the plasma grafting. The morphology of these composite materials were studied in detail in Refs. [27]. Here, Figure 2 shows only a representative image of these kinds of materials.

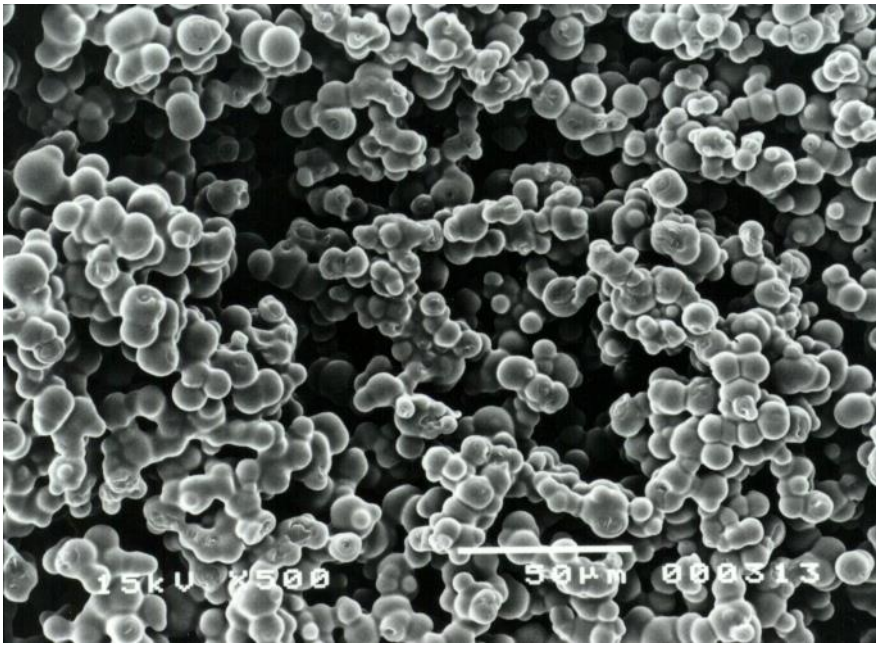

Figure 2. SEM micrograph of a cross-section of reinforced plasma-polymerised poly(2-hydroxyethyl acrylate) (*pl*PHEA) showing *pl*PHEA layer around the PMMA microspheres.

3.2. Thermal transition diagrams of water/PHEA and water/plPHEA

The DSC thermograms on heating and on cooling of bulk PHEA and the *pl*PHEA present in PMMA-*gr*-*pl*PHEA(28.7%) with different water mass fractions are shown in Figures 3 and 4 respectively. Bulk PHEA with water concentrations up to 0.2 shows only, on cooling and heating a single transition, which corresponds to the glass

transition of the hydrogel. Nevertheless, this range of water concentration decreases down to 0.15 for *pl*PHEA. Water crystallises on cooling from $\omega' = 0.3$ for bulk PHEA and from $\omega' = 0.2$ for *pl*PHEA.

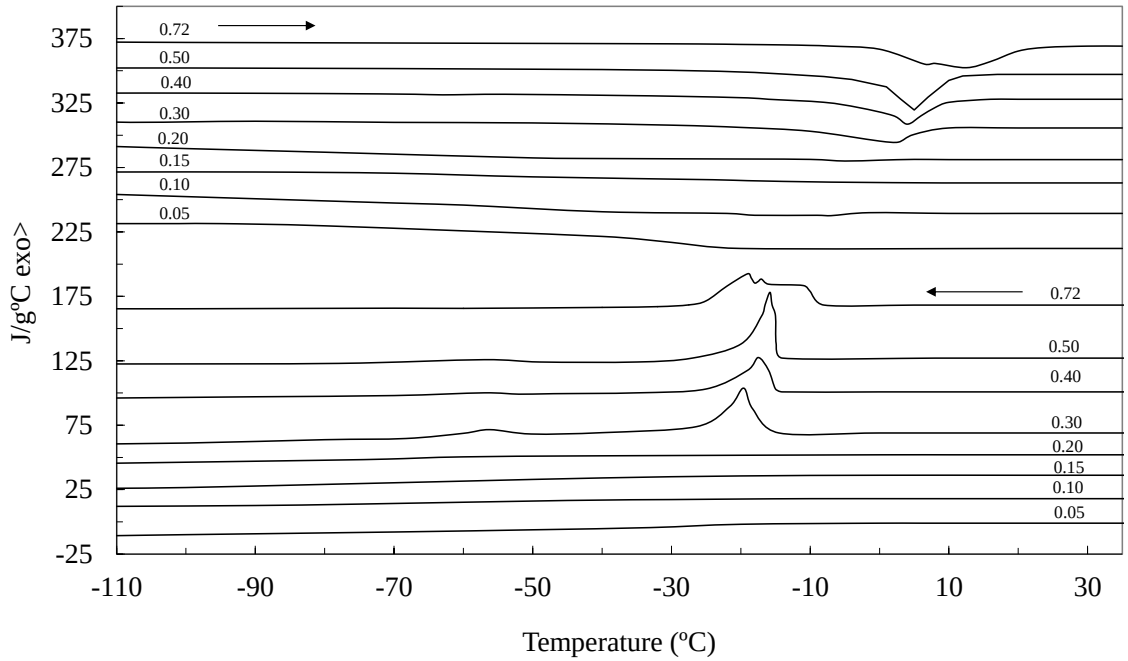

Figure 3. DSC thermograms at a heating (→) and cooling (←) rate of 10°C/min of bulk PHEA with different water mass fractions (ω'=0.05, 0.10, 0.15, 0.20, 0.30, 0.40, 0.50 and 0.72). Exothermic heat flow calculated per gram of water.

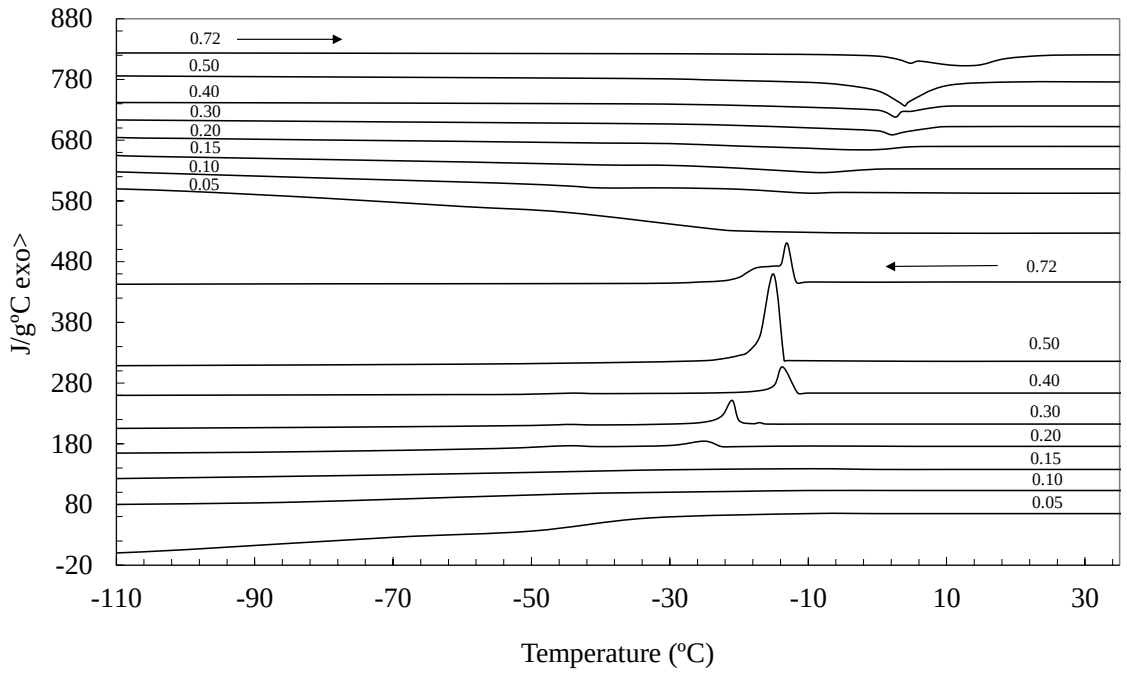

Figure 4. DSC thermograms at a heating (→) and cooling (←) rate of 10ºC/min of the *pl*PHEA present in the macroporous structure of PMMA (sample PMMA1/70E-*gr*-*pl*PHEA(28.7%)) with different water mass fractions (ω'=0.05, 0.10, 0.15, 0.20, 0.30, 0.40, 0.50 and 0.72). Exothermic heat flow calculated per gram of water.

3.3. Kinetics of water crystallisation for high and low water contents.

The DSC heating scans of bulk PHEA with high water mass fractions (ω' = 0.3) following experience A and B for T_{hold} = -10, -30, -50, -60 and –65 are shown in Figure 5. It can be observed a very different behaviour depending on the thermal method followed in this kind of PHEA. However, the DSC heating scans of *pl*PHEA present in PMMA1/70E-*gr*-*pl*PHEA(28.7 wt.%) with high water mass fractions (ω' = 0.3) following experience A and B for T_{hold} = -10, -30 and –50 show hardly no difference between the two thermal methods as it can be seen in Figure 6.

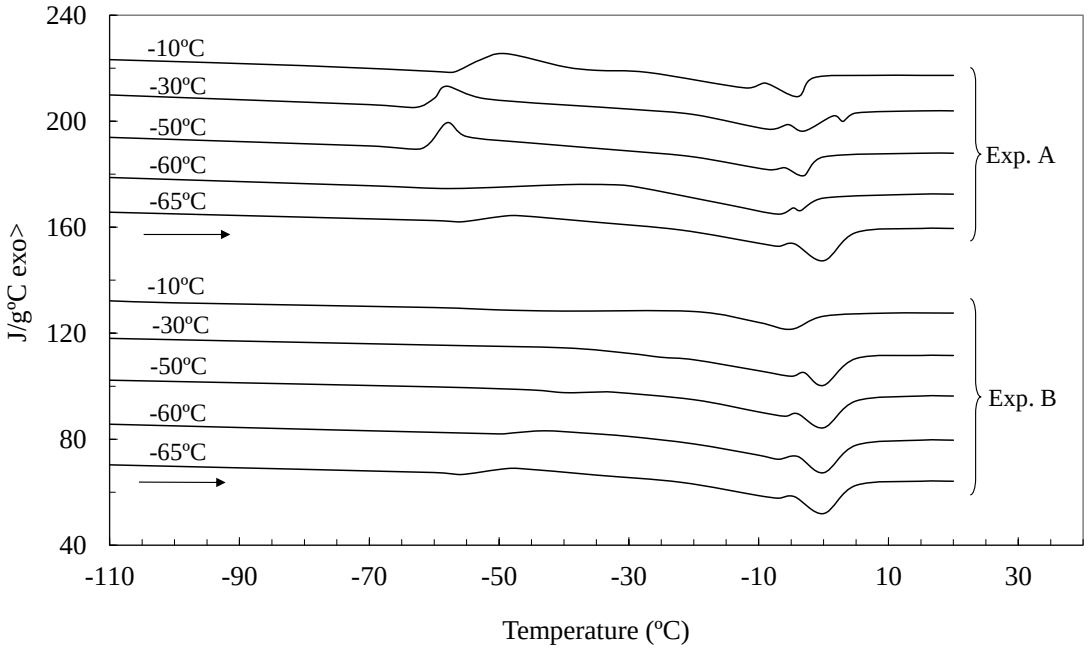

Figure 5. DSC heating scans of bulk PHEA with high water mass fractions (ω' = 0.3) following experience A and B for T_{hold} = -10, -30, -50, -60 and -65ºC. Exothermic heat flow calculated per gram of water.

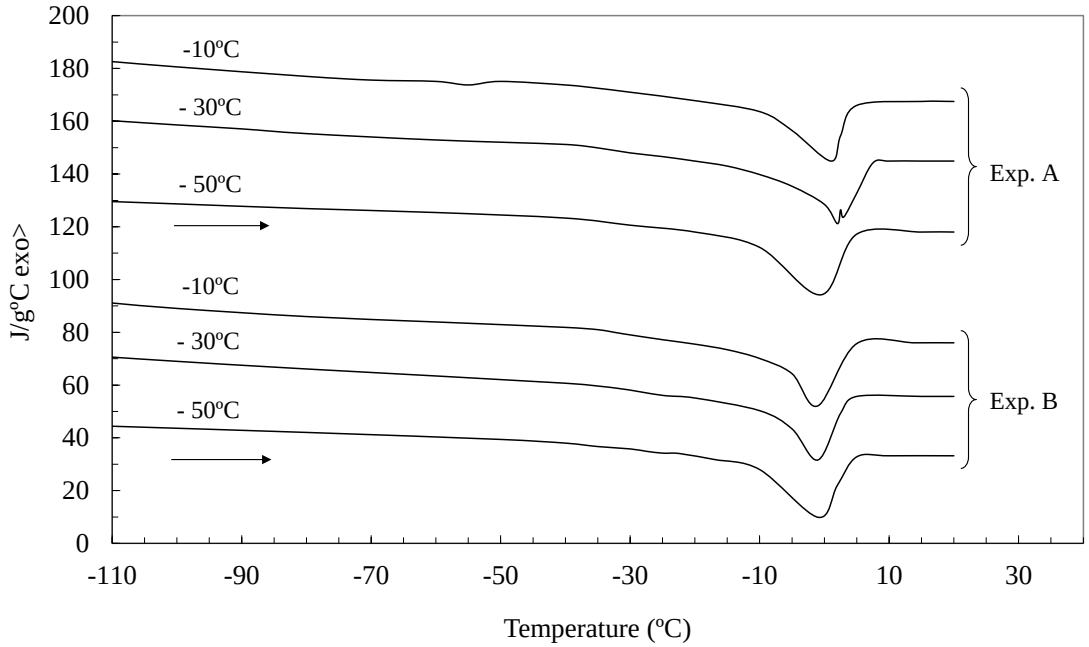

Figure 6. DSC heating scans of *pl*PHEA present in PMMA1/70E-*gr*-*pl*PHEA(28.7 wt.%) with high water mass fractions (ω' = 0.3) following experience A and B for T_{hold} = -10, -30 and -50ºC. Exothermic heat flow calculated per gram of water.

The results of kinetics for water crystallisation for low water contents are shown in Figure 7 and 8. Bulk PHEA and PMMA1/70E-*gr*-*pl*PHEA(28.7%) were swollen in liquid water to obtain a water mass fraction ω'=0.10. This low water mass fraction belongs to the first domain ($\omega' < \omega'^{**}$) and only the glass transition of the swollen hydrogel without any sign of water crystallisation is seen on cooling. Only the glass transition of the swollen network is also seen on heating in the same interval, shifting towards lower temperatures as water mass fraction increases, without any sign of first-order phase transitions of water. Thus, all water remains non-crystallisable for this water mass fraction. Nevertheless, in the experiments now under consideration, it was demonstrated that holding at -30ºC during a certain amount of time, crystallisation of water becomes possible. In addition, the longer isothermal step at T_{hold}=-30ºC, the

more water crystallises. The total amount of water that crystallises was calculated through the melting enthalpies of the heating scans. The first and second DSC heating scans from -50 to 10ºC after holding at -30ºC during several times (0, 1, 2, 16.7, 33.3 and 61.7 hours) for bulk PHEA with low water mass fractions ($\omega' = 0.1$) are shown in Figure 7. The second heating scans from show smaller peaks of melting but they follow the same tendency. The same type of DSC heating scans for *pl*PHEA is shown in Figure 8. Since no sign of water melting for 1 hour of holding time at -30ºC, only the first DSC heating scans for 2 or more hours are shown. In the same way, only the second DSC heating scans for 16.7, 33.3 and 61,7 hours are shown due to no sign of melting was found from 0 to 33.3 hours of holding time. These results show that much less water crystallises in *pl*PHEA and more time is necessary to hold at –30ºC to crystallise water.

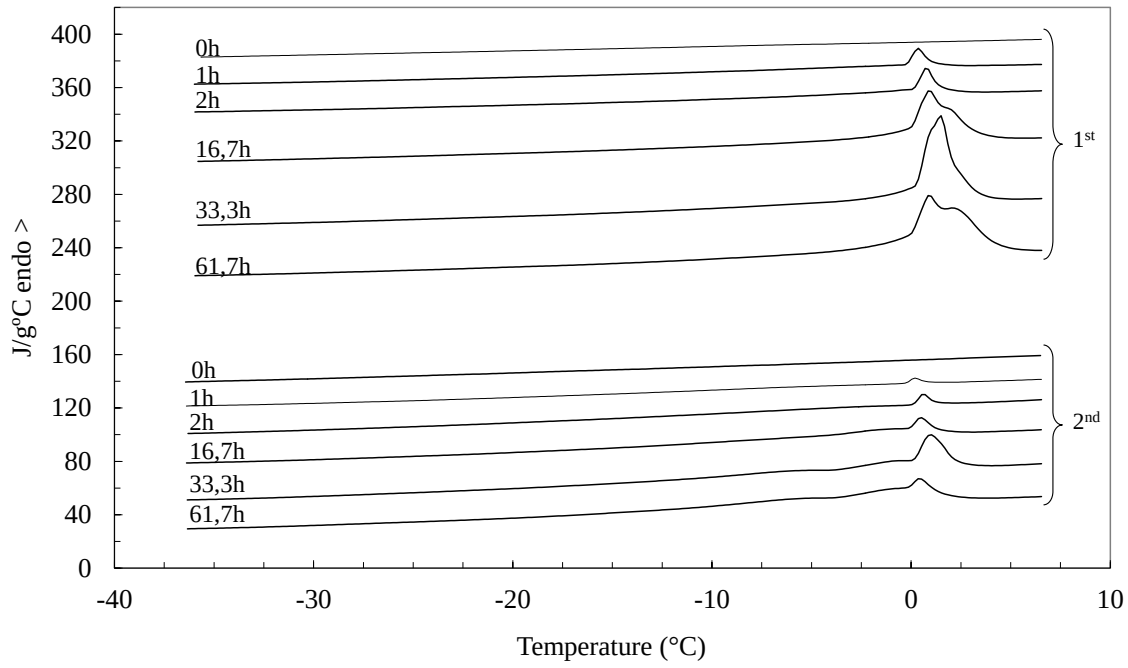

Figure 7. First and second DSC heating scans from -50 to 10ºC after holding at -30ºC during several times (0, 1, 2, 16.7, 33.3 and 61.7 hours) for bulk PHEA with low water

mass fractions (ω' = 0.10). Exothermic heat flow calculated per gram of water.

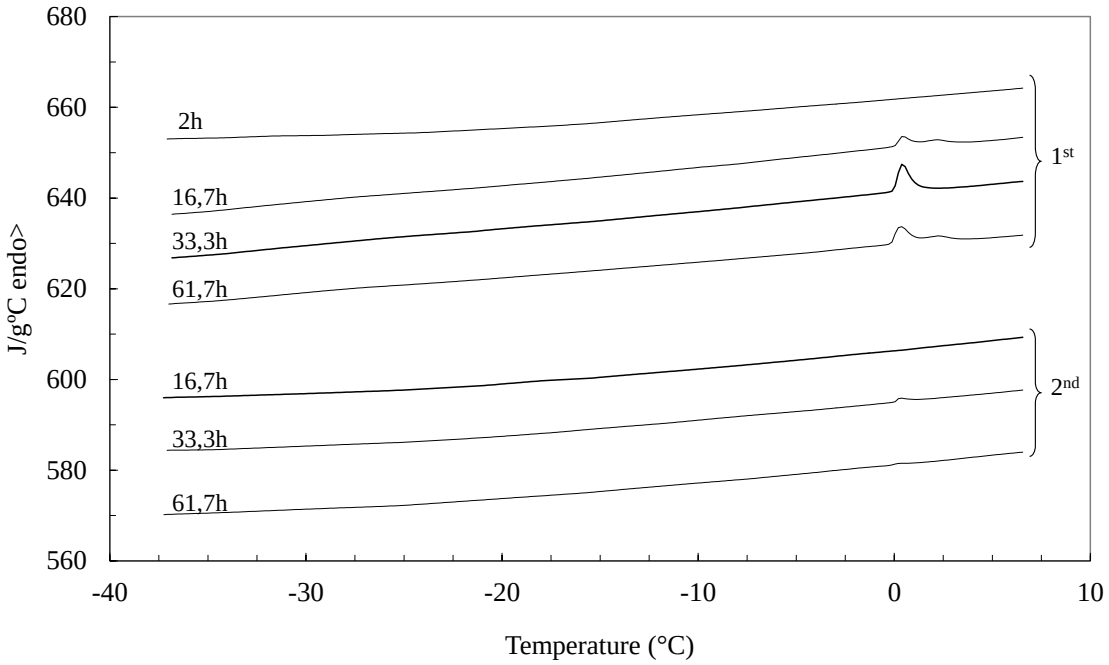

Figure 8. First and second DSC heating scans from -50 to 10ºC after holding at -30ºC for several times (2, 16.7, 33.3 and 61.7 hours) of the *pl*PHEA present in PMMA1/70E-*gr*-*pl*PHEA(28.7%) with low water mass fractions (ω' = 0.10). Exothermic heat flow calculated per gram of water.

4. Discussion

Three DSC thermograms can be selected from Figure 3 for bulk PHEA to observe the three water concentration domains. The bulk PHEA sample with ω'=0.05 is representative of the thermograms in which only the glass transition is observed both on cooling and heating. At intermediate water mass fractions (ω'=0.2) only the glass transition is observed on cooling. In the subsequent heating scan, contrary to what expected, there is not a clear crystallisation peak. However, there is a clear melting of water, which must has crystallised before on heating because no sign of crystallisation

appears on cooling as expected. Finally, for high water mass fractions (ω'=0.3), water crystallises on cooling appearing two crystallisation peaks. The first sharp peak at higher temperatures corresponds to free water and the second one at lower temperatures due to the crystallisation of water homogeneously mixed with the hydrogel. For these water concentrations, glass transition is no longer visible due to the other thermal transitions. However, a change in the baseline from the start to the end can be identified.

Three DSC thermograms can be also selected from Figure 4 to observe the three water concentration domains in the *pl*PHEA. In this case, at intermediate water mass fractions (ω'=0.15), a crystallisation exotherm is clearly seen on heating after the cooling scan in which only the glass transition is shown. All water remains non-crystallisable as well for *pl*PHEA in the first concentration domain ($\omega' < \omega'^{**}$). Thus, only the glass transition of the swollen network appears both on cooling and heating. For water mass fractions $\omega'^{**} < \omega' < \omega'^{*}$, no crystallisation is seen on cooling. Finally, for water mass fractions higher than ω'^{*}, water crystallises on cooling showing two crystallisation peaks as bulk PHEA. This second peak is much smaller than the first one. This means that at room temperature, before the start of cooling, phase separation takes place between pure water and swollen polymer domains. Water domains crystallise at a temperature close to that of pure water whereas the crystallisation from the homogeneous mixture of polymer segments and water molecules take place at a lower temperature. The amount of bulk water at high water mass fractions can be much higher than that of water mixed with polymer segments.

The temperature-composition diagram for each kind of PHEA can be drawn from the series of DSC thermograms (Figure 3 and 4) representing the crystallisation,

melting and glass transition temperatures as a function of water mass fraction (see Figure 9).

(a)

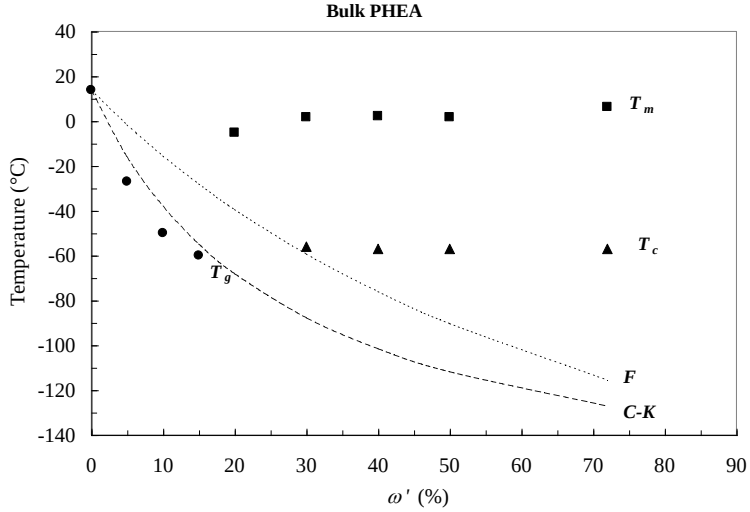

(b)

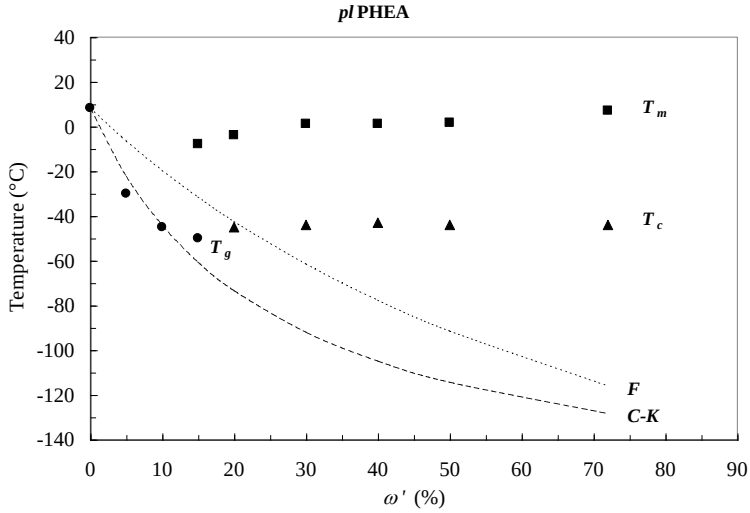

Figure 9. Experimental temperature-composition diagram of swollen bulk PHEA (*a*) and swollen *pl*PHEA present in macroporous PMMA (sample PMMA1/70E-*gr*-*pl*PHEA(28.7%)) (*b*): glass transition temperature on heating (T_g) (●), melting temperature of water on heating (T_m) (■), crystallisation temperature on cooling of water homogeneously mixed with the hydrogel (T_c) (▲), glass transition temperature

predicted by the Fox equation (*F*) (---) and the Couchman-Karasz equation (*C-K*) (———).

The temperature of the inflection point of the heating thermogram was taken to determine the glass transition temperature (T_g). The temperature of the maximum of the melting peak appearing on heating was taken to determine the melting temperature of water (T_m). The temperature of the maximum of the crystallisation peak, which appears on cooling at lower temperature and is related to water homogeneously mixed with the hydrogel, was taken to obtain the crystallisation temperature of water (T_c) in the temperature-composition diagram. These temperature-composition diagrams show that there is less undercooling of water crystallisation in the *pl*PHEA present in the PMMA-*gr*-*pl*PHEA(28.7%) composite material than in bulk PHEA. The origin of the liquid curve T_m , in a polymer-water system comes from the equality of the chemical potential of water in the hydrogel and in the crystalline state. Using the Flory-Huggins lattice model one obtains [11]:

$$\frac{1}{T_m} - \frac{1}{T_0} = \frac{-\Re}{\Delta H_m}\left\{\ln(1-\phi_d) + \phi_d + \overline{\chi}\phi_d^2\right\} \qquad (1)$$

Therefore, the T_m curve depends on the Flory-Huggins parameter and since bulk PHEA and *pl*PHEA differ chemically, this explains the discrepancies found between the undercooling of the two hydrophilic systems.

The values of ω'^{**} and ω'^{*} are often obtained from direct inspection of the transition diagram. To determine ω'^{**} and ω'^{*}, the experimental T_m and T_c curves must be extrapolated to lower concentrations to obtain the intersection with the T_g curve

respectively. However, it must be taken into account that at these low concentrations, the T_m and T_c curves are almost vertical [29-31]. Unfortunately, this zone is not experimentally accessible in our systems and it is not possible to determine these values with this method. Nevertheless, from direct inspection, according to the thermal transitions observed in the cooling and heating DSC thermograms performed with different water mass fractions (Figure 3 and 4), an approximate value of ω'^{**} and ω'^{*} can be determined calculating the mean of the water mass fractions of the DSC thermograms which are close to the exact value. Thus, the values determined for bulk PHEA were $\omega'^{**}\approx 0.17$ (mean value of ω'=0.15 and 0.20) and $\omega'^{*}\approx 0.25$ (mean value of ω'=0.20 and 0.30). Therefore, water remains always homogeneously mixed with the hydrogel phase for water mass fractions lower than 0.17, water does not crystallise on cooling but does so on heating for compositions between 0.17 and 0.25 and first order transitions are present both on cooling and on heating for water mass fractions higher than 0.25. These values are very close to those obtained in reference [15] for bulk PHEA polymerised with 1 wt.% of ethylene glycol dimethacrylate (EGDMA) ($\omega'^{**}\approx 0.20$ and $\omega'^{*}\approx 0.30$).

In the same way, for *pl*PHEA, analysing the cooling and heating DSC thermograms: $\omega'^{**}\approx 0.12$ (mean value of ω'=0.10 and 0.15) and $\omega'^{*}\approx 0.17$ (mean value of ω'=0.15 and 0.20). These results are shown in Table 1.

Sample	**ω'****	**ω'***
Bulk PHEA	0.17	0.25
*pl*PHEA	0.12	0.17

Table 1. Critical water mass fractions of bulk PHEA and *pl*PHEA present in sample PMMA1/70E-gr-plPHEA(28.7%).

For water mass fractions $\omega' < \omega'^{**}$, only the glass transition of an amorphous polymer-solvent system occurs in both PHEA systems (see figures 3 and 4) because most water remains as bound water decreasing the glass transition temperature with increasing the water mass fraction. This decrease gets greater in bulk PHEA than in *pl*PHEA even though the glass transition temperature in the dry state is lower for the plasma polymer. Thus, for ω'=0.15 the glass transition is -60˚C and -50 ˚C for of bulk PHEA and *pl*PHEA respectively (see figure 9) showing more presence of bound water in the bulk polymer. Furthermore, for a water mass fraction of ω'=0.2, the melting temperature of bulk PHEA is -5,2˚C, lower than that of *pl*PHEA (-3,9 ˚C) showing greater presence of freezable bond water. However, from ω'=0.3 on, water shows a phase transition as free water, with a certain supercooling of a few degrees, close to that of bulk water in both PHEA systems.

The glass transition temperature curve predicted by the Fox and Couchman-Karasz equations were determined with T_{gw} =134 K and $\Delta c_{pw}(T_g)$ = 1.94 *J/gK* [32]. These values of bulk PHEA (T_{g0} = 287 K and Δc_{p0} = 0.42 *J/gK*) and those of the *pl*PHEA present in the PMMA-*gr*-*pl*PHEA(28.7%) sample (T_{g0} = 281.4 K and Δc_{p0} = 0.39 *J/gK*) were determined from the DSC thermograms of the xerogels (Δc_{p0} = 0.112·100/28.7=0.39 *J/gK*). The prediction of Fox equation is far from the experimental results in both types of PHEA but the Couchman-Karasz equation fits very well the experimental results and supports the hypothesis of a homogeneous mixture water/polymer as the basic physical picture of a hydrogel.

Kinetics for high water contents was studied following two thermal methods to study the influence of performing or not an extensive nucleation and growth in bulk

PHEA and *pl*PHEA with high water contents. The main difference between the two experiences is the total time that the samples stay at a temperature lower than T_c in the whole experience. The more time the samples are at temperatures lower than T_c, the more nucleation and growth are expected to occur. For bulk PHEA with $\omega' = 0.3$, when T_{hold} = -10ºC, the temperature of the sample is hold at a temperature higher than T_c and the last heating scan of experience A shows a strong crystallisation peak followed by a melting peak (see Figure 5) because only nucleation without crystal growth occurs in this experience. However, the same thermal treatment cooling down to -120ºC at 10 K/min instead of quenching did not show this strong crystallisation peak on heating because most water had crystallised before on cooling (see Figure 5). The sample spends much more time at a temperature lower than T_c in experience B and only a melting peak appears on the last heating scan of experience B. Most water crystallises before due to the extensive nucleation and growth obtained with this thermal treatment. The same behaviour is observed when T_{hold} is also higher than T_c (T_{hold} = -30 and -50ºC). However, both heating scans start looking the same for T_{hold} = -60, although less crystallisation of water appears still in experience B. Now, T_{hold} is lower than the crystallisation temperature (T_c). Finally, from T_{hold} = -65ºC on, both heating scans are exactly the same for experiences A and B. The same amount of water crystallises on heating in both experiences A and B. Nucleation always occurs at low temperatures independently of having crystallisation or not in the cooling scan. Experience B shows the crystallisation capacity at different temperatures once nucleation is produced. Holding during 15 minutes at temperatures between -10 and -50ºC clearly makes water to crystallise in bulk PHEA and practically there is not residual crystallisation on the subsequent heating scan. However, when T_{hold} is from -60 to -70ºC, crystallisation is slower and water does not crystallise completely holding at this temperature for 15

minutes. Water begins to crystallise on the following heating scan from T_{hold} showing clearly its existence. Experience A shows the nucleation capacity at different temperatures. Water does not crystallise or only a small amount does during all the thermal steps before the last heating scan from -120ºC to 20ºC in spite of holding during 15 minutes at T_{hold}. The shape of the crystallisation peak appearing on the heating scan is related to the kinetics of crystallisation, which enormously depends on the number of nucleus of crystallisation. The more number of nucleuses, the faster is the growth process of the water mass crystallised in bulk PHEA and this gives a higher initial slope of the exothermic peak. Thus, this slope significantly increases when T_{hold} decreases from -10 to -50ºC. However, from -50 to -70ºC, this slope markedly decreases. This gives an idea of the form of the distribution graph of the nucleation velocity of water in the mixture with the polymer segments with a maximum around -50ºC. The probability of occurring also crystal growth during the isotherm step for 15 minutes could be analysed with the areas of the crystallisation peaks appearing on heating but it clearly seems to be very small. The samples always spend more time at low temperatures in experience B. The lower T_{hold}, the shorter difference of time spent by the samples at low temperatures in experiences A and B. When T_{hold} is -10ºC, the samples spend much more time at low temperatures in experience B. For this reason, the thermograms of these two thermal treatments are very different occurring extensive nucleation and crystal growth in experience B before the last heating scan.

The same thermal treatments were performed with sample PMMA1/70E-*gr*-*pl*PHEA(28.7 wt.%) with ω' = 0.3. The last heating scan of the experience A shows crystallisation on heating followed by a melting peak when T_{hold} = -10ºC for *pl*PHEA (see Figure 6). This crystallisation peak is much smaller than that found for bulk PHEA.

No crystallisation peak appears on heating in experience B, only a melting peak. A similar behaviour is observed when T_{hold} is still higher than the crystallisation temperature (T_{hold} = -30ºC). Experience A shows a slight crystallisation on heating followed by a strong melting peak for *pl*PHEA. The temperature-composition diagrams showed that there is less undercooling of water crystallisation in the *pl*PHEA than in bulk PHEA (see Figure 9). For this reason, T_{hold} is lower than T_c when T_{hold} = -50ºC and exactly the same heating scan for experiences A and B are obtained (see Figure 6) as it occurred for T_{hold} = -65ºC in bulk PHEA. Thus, for T_{hold} = -60, -65 and -70ºC, exactly the same heating scans are obtained for experiences A and B. All these experiments show a clear difference between the kinetics of water crystallisation for high water contents in bulk PHEA and *pl*PHEA. Experience A shows that water crystallises very fast in *pl*PHEA. An appreciable crystallisation at the same time as nucleation occurs during the 15 minutes of the isothermal step. Although, a small amount of residual water crystallises on the last heating scan.

The first heating scans for bulk PHEA with low water contents show that the melting area of water increases with increasing holding time (see Figure 7). For these low water mass fractions (ω' = 0.10) lower than the critical concentration (ω'^{**} = 0.17), water cannot crystallise without the isothermal step at -30ºC. Figure 10 shows that an equilibrium value of crystallised water must be achieved after a certain amount of time.

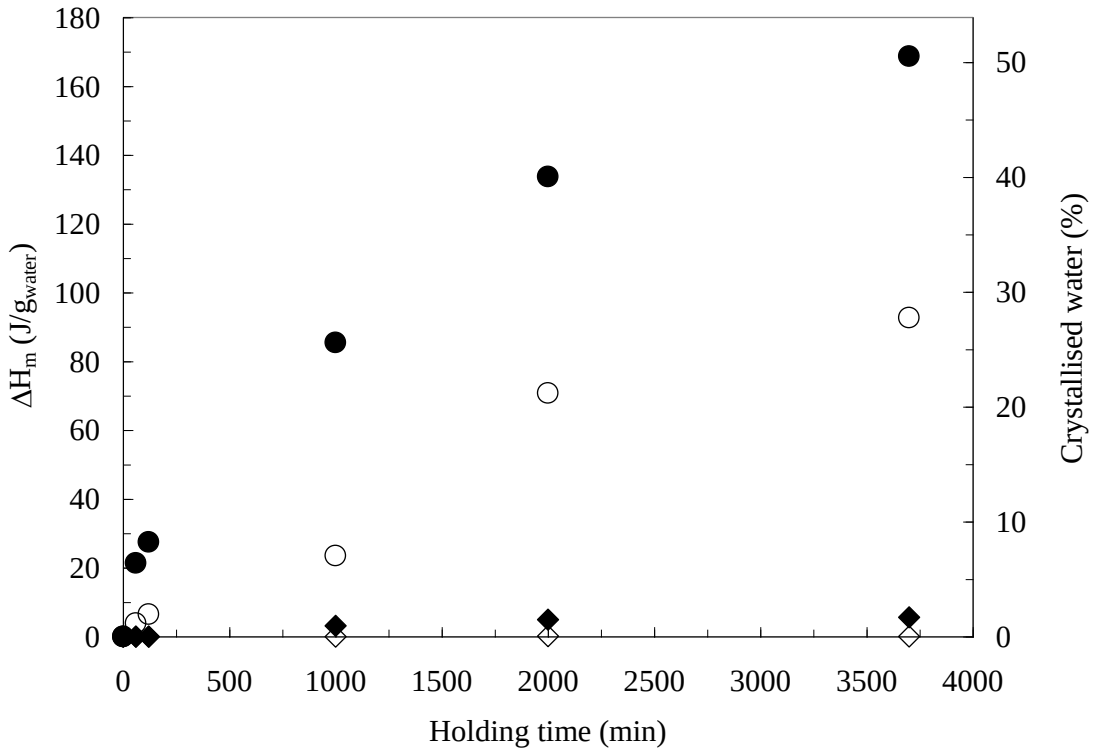

Figure 10. Melting enthalpy (ΔH_m) and wt.% of crystallised water as a function of the holding time at -30ºC after the first (solid symbols) and the second (open symbols) heating scans from -50 to 10ºC for bulk PHEA (○) and *pl*PHEA present in PMMA1/70E-*gr*-*pl*PHEA(28.7%) (◇) with low water mass fractions (ω' = 0.10).

Crystal nucleus are formed in the isothermal step at this low temperature and the longer is this step, the more nucleation and subsequent growth are obtained until a maximum equilibrium amount of water. All the melting peaks of water in bulk PHEA appear around 0ºC (see Figure 7). This unexpected result can be clearly understood because when the temperature is cooled down to -30ºC and kept at this temperature, water does not crystallise and is segregated from the water/PHEA mixture because the solubility of water in the PHEA hydrogel is lower at this temperature. This water melts around 0ºC as free water on the subsequent heating scan after the isothermal step. The second heating scans show smaller peaks of melting but they follow the same tendency

(see Figure 7). Less water crystallises because the second heating scan is performed right after the first one and it is only seen the free water that has not had enough time to mix homogeneously with the polymer matrix. If the sample is kept at 10ºC for a long time after the first heating scan, water has time to mix homogeneously with the hydrogel and no phase transition appears on the last heating scan, only the glass transition. Figure 10 shows the melting enthalpy and the amount of crystallised water as a function of the holding time at -30ºC after the first and the second heating scan from -50 to 10ºC for bulk PHEA with low water mass fractions (ω' = 0.10). The amount of crystallised water is around two times lower after the second heating. The same tendency of water crystallisation was observed in the *pl*PHEA present in the PMMA-*gr*-*pl*PHEA(28.7%) composite material. Nevertheless, much less water crystallises in this kind of PHEA and holding for 2 hours at -30ºC is not enough time to crystallise water. Figure 10 shows how the melting enthalpy of water also increases with increasing holding time for *pl*PHEA after the first heating scan. However, after the second scan, the amount of crystallised water is close to 0%. After the first heating scan, there is very little free water (1.48% after 33.3 hours) which has time to mix with the *pl*PHEA. For these low water mass fractions (ω' = 0.10), lower than the critical concentration (ω'^{**} = 0.12), water cannot crystallise without the isothermal step at -30ºC. However, this experiment demonstrates that when the temperature is cooled down to -30ºC and the sample is kept at this temperature for some time, crystallisation of water becomes possible again for this kind of PHEA even though having a water mass fraction lower than the critical one (ω'^{**}). In addition, the more time holding at -30ºC, the more amount of water crystallises and an equilibrium value of crystallised water must be achieved after a certain amount of time. All the melting peaks of water in *pl*PHEA appear also around 0ºC as free water (see Figure 9) because when the temperature is

cooled down to -30ºC and kept at this temperature, water is segregated from the water/*pl*PHEA mixture as it occurred with bulk PHEA. These results show a very important difference in the crystallisation of water for low water contents in bulk PHEA and *pl*PHEA. Much less amount of water is segregated from the water/*pl*PHEA mixture (1.68% after 61.7 hours) than from the water/bulk PHEA one (50.5% after 61.7 hours). This significant difference must be due to the influence of the hydrophobic polymer in the PMMA1/70E-*gr*-*pl*PHEA(28.7%) composite material.

5. Conclusions

The transition diagrams of water/PHEA and water/*pl*PHEA show less undercooling of water crystallisation in *pl*PHEA than in bulk PHEA. The kinetics of water crystallisation for high water contents in bulk PHEA and *pl*PHEA are quite different. Water crystallises much faster in *pl*PHEA than in bulk PHEA. When swollen bulk PHEA and swollen *pl*PHEA (both with $\omega' = 0.10$) are kept at -30ºC for some time, crystallisation of water becomes possible even though with this low water mass fraction no crystallisation can be observed in the cooling or heating DSC thermograms. Crystallisation occurs because water is segregated from the water/polymer mixture in the isothermal step at -30ºC. All the melting peaks of water in bulk PHEA and *pl*PHEA appear around 0ºC as free water. Much less water is segregated from the water-*pl*PHEA mixture (1.68% after 61.7 hours) than from the water-bulk PHEA one (50.5% after 61.7 hours) due to the influence of the hydrophobic polymer in the PMMA1/70E-*gr*-*pl*PHEA(28.7%) composite material.

Acknowledgement: This work was supported by a Marie Curie Host Fellowship and by the Spanish Science and Technology Ministry through the MAT2001-2678-C02-01 and MAT2002-04239-C03-03 projects.

References

[1] Pedley, D.G.; Tighe, B.J. British Polymer Journal 1979, 11, 130.

[2] Nakamura, K.; Hatakeyama, T.; Hatakeyama, H. *Polymer* **1983**, 24, 871.

[3] Burghoff, H.G.; Pusch, W. *J. Appl. Polym. Sci.* **1979**, 23, 473.

[4] Sivashinsky, N.; Tanny, G.B. *J. Appl. Polym. Sci.* **1981**, 26, 2625.

[5] Higuchi, A.; Komiyama, J.; Iijima, T. *Polym. Bull.* **1984**, 11, 203.

[6] Rault, J.; Gref, R.; Ping, Z.H.; Nguyen, Q.T.; Néel, J. *Polymer* **1995**, 36, 1655.

[7] Rault, J.; Ping, Z.H.; Nguyen, Q.T. *J. Non-Cryst. Solids* **1994**, 172/174, 733.

[8] Rault, J. *Macromolecular Symposia* **1995**, 100, 31-38.

[9)] Rault, J.; Lucas, A.; Neffati, R.; Pradas, M.M. *Macromolecules* **1997**, 30, 7866.

[10] Sánchez M.S., Ferrer G.G., Pradas M.M., Ribelles J.L.G. *Macromolecules* **2003**, 36, 860-866.

[11] Fox, T.G. *Bull. Am. Phys. Soc*. **1953**, 1, 123.

[12] Couchman, P.R. *Macromolecules* **1978**, 11, 1156.

[13] Couchman, P.R., *Macromolecules* **1987**, 20, 1712.

[14] Johari, G. P.; Hallbrucker, A.; Mayer, E.; *Nature* **1987**, 330, 552.

[15] Sánchez, M.S. In *On the nature of thermal transitions in acrylic polymer gels*. Ed. ProQuest Information and Learning Company, 2003.

[16] Hoffman, A.S. In *Hydrogels - a broad class of biomaterials.* In *Polymers in medicine and surgery*; Kronenthal, Oser, Martin, Eds.; Plenum Press: New York, 1975; p 33.

[17] Tanzawa, H.; Nagaoka, S.; Suzuki, J.; Kobayashi, S.; Masubuchi, Y.; Kikuchi, T. In *Cell adhesion and growth on the surface of synthetic hydrogels.* In *Biomedical polymers*; Goldberg, E., Nakajima, A.., Eds;. Academic Press, 1980; p 189.

[18] Peppas, N.A. Ed. In *Hydrogels in medicine and pharmacy*, vol. 3; Boca Raton, FL: CRC Press, 1987.

[19] Peppas, N.A. ; Langer, R. *Science* **1994**, 263-1715.

[20] Bell, C.L. ; Peppas N.A. *Adv Polym Sci* **1995**, 122-125.

[21] Stoy, V.; Kliment, C. In *Hydrogels: Speciality Plastics for Biomedical and Pharmaceutical Applications*; Technomic Publishers: Basel, 1996.

[22] Murayama, S.; Kuroda, S.I.; Osawa, Z. *Polymer* **1993**, 34, 2845-3893 .

[23] Eschbach, F. O.; Huang, S. J.; In *Interpenetrating Polymer Networks*; Klempner, D., Sperling, L.H., Utracki, L.A., Eds.; Advances in Chemistry Series 239; American Chemical Society: Washington, DC, 1994; Chapter 9.

[24] Ramaraj, B.; Radhakishman, G. *Polymer* **1994**, 35, 2167.

[25] Koenigs, M.M.E. ; Pal, A. ; Mortazavi, H.; Pawar, G.M. ; Storm, C.; Sijbesma, R.P. *Macromolecules* **2014**, 47, 2712-2717 .

[26] Cha, C.Y.; Shin, S.R.; Gao, X.G., Annabi, N.; Dokmeci, M.R.; Tang, X.W., Khademhosseini, A. *Small* **2014**, 10, 514-523.

[27] Aroca, A.S.; Pradas, M.M.; Ribelles, J.L.G. *Polymer* **2007**, 48, 2071-2078.

[28] Aroca, A.S.; Ribelles, J.L.G; Pradas, M.M.; Garayo, A.V.; Antón, J.S. *European polymer Journal* **2007**, 43, 4552-4564.

[29] Franks, F. In *Thermal Analysis*, vol 2; Hemminger, W., Ed, 1980.

[30] Mackenzie A. P., Rasmussen D. H., in (31). P. 146

[31] Yasuda, H.; Olf, H. G.; Crist, B.; Lamaze, C. E.; Peterlin, A. In *Water Structure at the Water-Polymer Interface*; Jellinek, H.H.G., Ed.; Plenum Press; New York, 1973.

[32] Johari, G.P.; Hallbrucker, A.; Mayer, E. *Nature* **1987**, 330, 552.

Figure Captions

Figure 1. Expected shapes of the cooling and heating scans for polymer-water systems with compositions ω'_1, ω'_2 and ω'_3 belonging to the three different concentration domains [32].

Figure 2. SEM micrograph of a cross-section of plasma-polymerised poly(2-hydroxyethyl acrylate) (*pl*PHEA) grafted onto macroporous poly(methyl methacrylate) (PMMA) showing *pl*PHEA layer around the PMMA microspheres.

Figure 3. DSC thermograms at a heating (a) / cooling (b) rate of 10ºC/min of bulk PHEA with different water mass fractions (ω'=0.05, 0.10, 0.15, 0.20, 0.30, 0.40, 0.50 and 0.72). Exothermic heat flow calculated per gram of water.

Figure 4. DSC thermograms at a heating (a) / cooling (b) rate of 10ºC/min of the *pl*PHEA present in the reinforced macroporous structure (sample PMMA1/70E-*gr*-*pl*PHEA(28.7%)) with different water mass fractions (ω'=0.05, 0.10, 0.15, 0.20, 0.30, 0.40, 0.50 and 0.72). Exothermic heat flow calculated per gram of water.

Figure 5. DSC heating scans of bulk PHEA with high water mass fractions (ω' = 0.3) following experience A and B for T_{hold} = -10, -30, -50, -60 and -65ºC. Exothermic heat flow calculated per gram of water.

Figure 6. DSC heating scans of *pl*PHEA present in PMMA1/70E-*gr*-*pl*PHEA(28.7 wt.%) with high water mass fractions (ω' = 0.3) following experience A and B for T_{hold} = -10, -30 and -50ºC. Exothermic heat flow calculated per gram of water.

Figure 7. First and second DSC heating scans from -50 to 10ºC after holding at -30ºC during several times (0, 1, 2, 16.7, 33.3 and 61.7 hours) for bulk PHEA with low water mass fractions (ω' = 0.10). Exothermic heat flow calculated per gram of water.

Figure 8. First and second DSC heating scans from -50 to 10ºC after holding at -30ºC

for several times (2, 16.7, 33.3 and 61.7 hours) of the *pl*PHEA present in PMMA1/70E-*gr-pl*PHEA(28.7%) with low water mass fractions (ω' = 0.10). Exothermic heat flow calculated per gram of water.

Figure 9. Experimental temperature-composition diagram of swollen bulk PHEA (a) and swollen plPHEA present in macroporous PMMA (sample PMMA1/70E-gr-plPHEA(28.7%)) (b): glass transition temperature on heating (Tg) (●), melting temperature of water on heating (Tm) (■), crystallisation temperature on cooling of water homogeneously mixed with the hydrogel (Tc) (▲), glass transition temperature predicted by the Fox equation (F) (---) and the Couchman-Karasz equation (C-K) (———).

Figure 10. Melting enthalpy (ΔH_m) and wt.% of crystallised water as a function of the holding time at -30ºC after the first (solid symbols) and the second (open symbols) heating scans from -50 to 10ºC for bulk PHEA (○) and *pl*PHEA present in PMMA1/70E-*gr-pl*PHEA(28.7%) (◇) with low water mass fractions (ω' = 0.10).

Tables

Table 1. Critical water mass fractions of bulk PHEA and *pl*PHEA present in sample PMMA1/70E-gr-plPHEA(28.7%).